Journal of Organometallic Chemistry 696 (2011) 3836–3845

Contents lists available at SciVerse ScienceDirect

Journal of Organometallic Chemistry

journal homepage: www.elsevier.com/locate/jorganchem

In vitro binding studies of organotin(IV) complexes of 1,2-bis(1H-benzimidazol-2-yl)ethane-1,2-diol with CT-DNA and nucleotides (5′-GMP and 5′-TMP): Effect of the ancillary ligand on the binding propensity

Farukh Arjmand*, Fatima Sayeed, Shazia Parveen

Department of Chemistry, Aligarh Muslim University, Aligarh, UP 202002, India

ARTICLE INFO

Article history:
Received 11 May 2011
Received in revised form
9 August 2011
Accepted 14 August 2011

Keywords:
Organotin(IV) complexes
DNA binding
5′-GMP & 5′-TMP
Circular dichroism

ABSTRACT

The chiral benzimidazole ligand, 1,2-Bis(1H-benzimidazol-2-yl)ethane-1,2-diol, **L**, exhibiting coordination mode with an oxygen atom of alcohol group directed towards the metal ion and another –OH group with different molecular axis directed away from the metal center was utilized as a building block for organotin complexes [$C_{18}H_{19}N_4O_2SnCl$], [$C_{28}H_{23}N_4O_2SnCl$] and [$C_{52}H_{42}N_4O_2Sn_2$] (**1**–**3**). Complexes **1** and **3** exhibit a pentacoordinate geometry while the complex **2** reveals hexacoordinated environment around the Sn(IV) metal ions as evidenced by ^{119}Sn NMR studies. The DNA binding ability of benzimidazole ligand and their organotin(IV) complexes **1**–**3** were examined by employing different biophysical methods. The absorption titration of the complexes with CT-DNA reveal significant hyperchromic effect together with strong bathochromic shift of 4–5 nm which infer substantial binding of the complexes with CT-DNA. The intrinsic binding constant K_b values of the complexes **1**–**3** were found to be $2.16 \pm 0.04 \times 10^4$, $3.47 \pm 0.04 \times 10^4$ and $4.60 \pm 0.04 \times 10^3$ M^{-1}, respectively, suggesting pronounced binding of complex **2** with DNA double helix. The mechanism of binding of the complexes was further ascertained by the interaction studies of these complexes with nucleotides (5′-GMP and 5′-TMP) using absorption spectroscopy suggesting a clear preference for 5′-GMP binding which was further authenticated by NMR (^{1}H and ^{31}P NMR) studies.

1. Introduction

Spectacular success of cisplatin, cis-diamminedichloroplatinum(II) [1], an archetypical inorganic drug for treating solid cancers led to the discovery of many other second generation drugs such as oxaliplatin, carboplatin, picoplatin, etc., however owing to the limitations of platinum drugs, such as severe side effects, intrinsic and extrinsic resistance; and also since cancers are derived from numerous tissues with new multiple etiologies, therefore, these compounds cannot be potent (cytotoxic) against different the phenotypes of tumors [2], thus a resurging need for the developing new non-platinum metal compounds was realized. In the forefront on therapeutic regime are organotin compounds which have since 1972 demonstrated their cytotoxic activity (one compound triphenyltin acetate was shown to retard tumor growth in mice while its chloride derivative did not show any potency) [3]. Since then, a large number of organotin derivatives have been prepared and tested *in vitro* and *in vivo*, against murine leukemia cell lines [4]. Recent reports in literature reveal synthesis of many organotin metal complexes and their DNA binding studies [5–8]. Most of the compounds tested earlier exhibited interesting activity in specific cancer models, but often lacked activity against broad spectrum of experimental tumors. Nevertheless, there is possibility for variation of organic moieties and donor ligands linked to metal which can result in several organotin with high antitumor activity [9]. The ligand framework plays a significant role in metal-based pharmaceuticals via alteration in the biological properties by modifying reactivity or substitution inertness [10]. The effects of varying substituents of organotin(IV) metal ions both aliphatic and aromatic were studied as it is well known that the biological effects of organotins depends on both the nature and number of organic groups bound to Sn(IV) cation.

Besides this, introduction of an element of chirality is an attractive prospect as it could enhance the pharmacological uptake of the drug entity by adopting specific conformation and stereoselective binding with molecular target DNA [11]. We have been interested in a chiral tridentate ligand 1,2-Bis(1H-benzimidazol-2-yl)ethane-1,2-diol, as it is a versatile tridentate facially coordinating

* Corresponding author. Tel.: +91 5712703893.
E-mail address: farukh_arjmand@yahoo.co.in (F. Arjmand).

0022-328X/$ – see front matter © 2011 Elsevier B.V. All rights reserved.
doi:10.1016/j.jorganchem.2011.08.007

ligand and substituted benzimidazoles have shown diverse and broad spectrum of activities, antihistamine [12], antiulcerative [13], anti-inflammatory, analgesic [14], antioxidant [15], antibacterial [16], antitumor [17], antiproliferative [18], etc. These benzimidazoles selectively inhibit endothelial cell growth and suppress angiogenesis *in vitro* and *in vivo* [19]. Since DNA has been identified as the primary molecular target of metal-based anticancer drugs, interaction of metal complexes with DNA ascertains the extent and mode of DNA binding and the potential of these complexes to act as chemotherapeutic agents. There are various modes of DNA interactions broadly, covalent, non-covalent, intercalation, etc. [20]. DNA targeted metal-based drugs which involve covalent binding to nucleobase moieties have shown low degree of selectivity. On the other hand, non-covalent DNA binding metal complexes are known to strongly influence DNA binding properties and among them organotin is the prominent class of compounds exhibiting non-covalent binding mode [21,22]. To evaluate the effect of ancillary ligand as well as organic substituents on the binding properties of organotins, we have incorporated three organotins viz. dimethyltin dichloride, diphenyltin dichloride and triphenyltin chloride in the benzimidazole ligand scaffold and studied their DNA propensity by various biophysical spectroscopic methods (viz. UV titrations, fluorescence titrations and circular dichroism) and viscosity measurements. Furthermore, specific mode of binding exhibited by the complexes was ascertained by nucleotide recognition of these complexes with 5′-GMP and 5′-TMP using electronic absorption and NMR techniques.

2. Results and discussion

2.1. Infrared spectroscopy

In the IR spectra of the ligands the −OH and −NH frequencies are present as a broad envelope in the region from 3450 to 3199 cm^{-1} due to intermolecular hydrogen bonding NH and OH groups [21,23] which display minor changes on complexation. However, a medium or relatively weak band at 1623 cm^{-1} with a small shoulder at 1536 cm^{-1} corresponding to ν(C═N) in the IR spectra of the ligands [24] were considerably shifted by 2–3 cm^{-1} and become larger and sharper indicating the involvement of the nitrogen atom in complexation with Sn(IV) metal ion in all the complexes **1**–**3**. Other frequencies in complexes corresponding to ν(Sn−C), ν(Sn−N), ν(Sn−O) and ν(Sn−Cl) appeared at 557–588, 435–446, 517–546 and 279–256 cm^{-1}, respectively [25–27].

2.2. Nuclear magnetic resonance spectroscopy

The conclusions drawn from the ^{1}H NMR spectrum of free ligand were extrapolated to the complexes **1**–**3** owing to the data similarity. In complex **1**, the characteristic peak of the methyl groups attached to the tin is observed at 0.7–1.9 ppm [28]. While in complexes **2** and **3**, the presence of Sn−Ph protons at 7.8 and 7.9 ppm [29] confirms the formation of the complexes. The ^{1}H NMR spectra of all the complexes revealed a resonance for the CH proton attached to the hydroxyl group at 5.9–5.8 ppm which was shifted downfield compared to the free ligand at 5.4 ppm [30] showing the involvement of adjacent hydroxyl group in complexation with tin metal ion. The most striking difference in the ^{1}H NMR of complex **3** with the other complexes **1** and **2** was the disappearance of the hydroxyl protons of ligand at 6.4 ppm concomitant with the formation of complex in 1:2 stoichiometric ratio [30]. The aromatic protons of the ligand appear as a multiplet in the range of 7.1–7.5 ppm. In addition, due to rapid exchange between the two nitrogen atoms of imidazole ring, the NH protons of the ligand were not observed in the NMR spectra. This observation was in accordance with the earlier reports [31,32].

The ^{13}C NMR spectra of the ligand exhibit signals corresponding to C═N, C−O at 155 and 68–70 ppm, respectively [30] which were shifted in the downfield in the complexes. In addition, the complex **1** displays the methyl carbons attached to the tin metal ion (Sn−CH_3) at 10–14 ppm; the other complexes **2** and **3** exhibited only one set of NMR signals for both the phenyl groups (Sn−Ph) and for the ligands from 127 to 136 ppm, which provide evidence for the magnetic equivalence of both the phenyl groups of the ligands and the complexes on the NMR time scale [33,34].

In order to provide further evidence to establish the structure of the complexes in solution [35], ^{119}Sn NMR spectra was recorded (Fig. 1). It is well known that ^{119}Sn chemical shifts are very sensitive to change in the coordination number of tin and to the nature of groups directly attached to the tin atom [36]. The chemical shift values for the complexes reported here are within the expected range for the complexes **1** and **2** (−186 and −222 ppm, respectively) with the coordination number of five while complex **3**

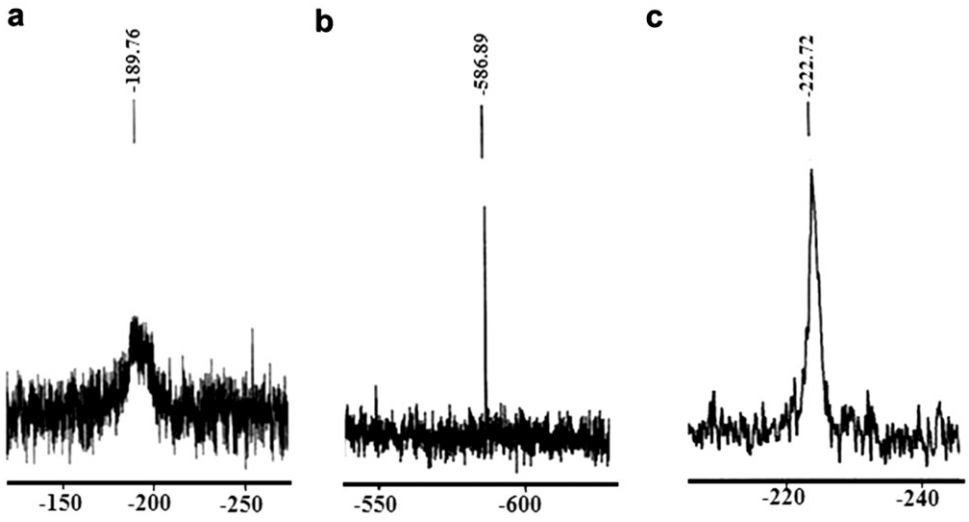

Fig. 1. ^{119}Sn NMR spectra of complexes (a) **1** (b) **2** and (c) **3**.

exhibits six coordinate geometry displaying a chemical shift value at −586 ppm [37].

2.3. Electronic absorption spectroscopy

The absorption spectra of the complexes **1**–**3** were recorded in methanol at room temperature and revealed bands at 207–210, 245, and 275 nm attributed to intraligand (IL) transitions of the ligands.

3. DNA binding studies

3.1. Absorption spectral studies

The absorption spectra of complexes **1** and **2** in presence and in the absence of CT-DNA are depicted in Fig. 2 (and for complex **3**, Supplementary Information fig. S1). In absence of CT-DNA, all the complexes exhibit similar absorption spectra with the peaks centered at 245 and 275 nm corresponding to n–π* and at 207–210 nm for π–π* IL transitions, respectively, owing to the presence of benzimidazole ligand scaffold. In presence of incremental amounts of CT-DNA, a significant hyperchromic effect with a strong bathochromic shift was observed for all studied complexes. Complex **2** displayed a significant bathochromic shift of 4–5 nm supports a higher degree of binding for this complex towards CT-DNA [38]. Thus, from these spectral changes, we deduce that the complexes bind to the CT-DNA by a strong electrostatic interaction mode as a result of a high affinity of cationic Sn(IV) to the polyanionic phosphate backbone and lack of base specificity in DNA binding. Literature reveals [39,40] strong Lewis acid Sn(IV) ions neutralize the negative charge of the CT-DNA thereby, causing contraction and conformational changes in the CT-DNA via electrostatic interaction with the phosphate backbone of DNA double helix. The spectral features reveal that the complex **2** has much higher affinity towards CT-DNA among the other complexes which could be attributed to the presence of labile groups of varying steric demand and hydrophobicity thereby, facilitating multifaceted binding modes. The hydrophobic phenyl groups leads to more intimate binding and possibly promoting partial insertion of the complex **2** into the DNA helix. In addition, hydrolysis of labile chloride atoms in the complex **2** [41] and hard Lewis acidic property of Sn(IV) together contribute to the vicinal electrostatic binding of complex with the polyanionic phosphate backbone of CT-DNA [42]. Furthermore, the presence of −OH group in the ligand being out of the planar phenyl rings, as validated by the crystal structure of the ligand [30] forms hydrogen bonds with DNA. Although complete intercalation between a set of adjacent base pairs is sterically prohibited, but some type of partial intercalation can be envisioned for complex **2**. Similarly, complex **1** also exhibit an electrostatic binding mode pertaining to presence of Sn(IV) central metal ion which substantiate preferential binding to the DNA phosphate backbone; the discerning binding exhibited by complex **1** compared to complex **2** is due to the absence of phenyl group in the complex. The complex **3** has steric constraints caused by the bulky phenyl groups of the triphenyltin(IV) moiety which accounts for its lower binding propensity with DNA. The K_b value calculated revealed that the comparative binding strength of the complexes with CT-DNA were in the order **2** > **1** > **3** (Table 1).

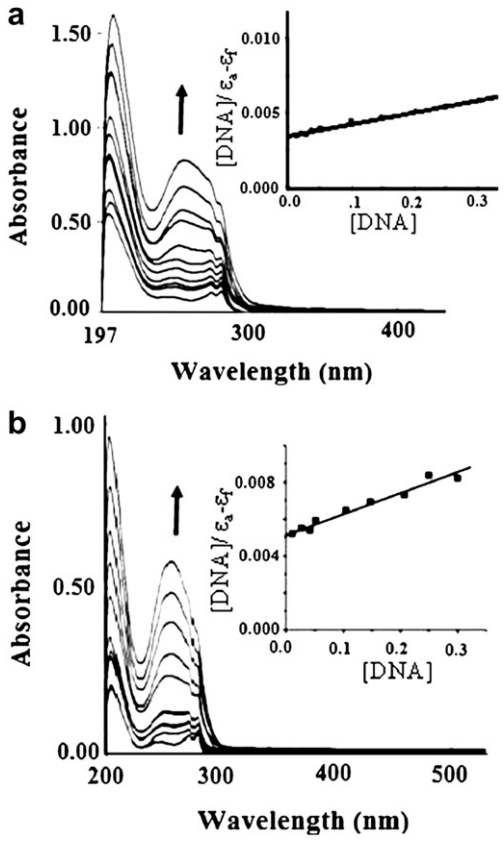

Fig. 2. Absorption spectra of complexes (a) **1** and (b) **2** in the presence of increasing amount of CT-DNA. Inset: Plots of [DNA]/(ε_a–ε_f) vs [DNA] for the titration of CT-DNA with complexes. [Complex] = 1.3 × 10^{-4} M, [CT-DNA] = 0–1.2 × 10^{-4} M.

3.2. Interaction studies with 5′-GMP and 5′-TMP

To avoid the macrostructural effects of larger nucleic acid which might obscure the fundamental biomolecular selectivity of these complexes, absorption titration with small nucleic acid fragments such as mononucleotides (5′-GMP and 5′-TMP) were performed under physiological conditions. Gellert et al. [43] demonstrated X-ray structural studies showing predominant binding of thirty binary and ternary mononucleotide-transition metal complexes by first two modes through exocyclic nitrogen atom of purine rings (N1 and N7 atom) and N3 of the pyrimidine and oxygen atom of the phosphate group present in the nucleotides. Later, extensive work on the interaction of organotin(IV) complexes DNA and nucleotides was also carried out by Yang et al. to elucidate the probable mode of binding of the Sn(IV) complexes [39,40]. The gradual addition of 5′-GMP/5′-TMP (0–0.50 × 10^{-4} M) to the metal complexes **1**–**3** leads to significant "hyperchromic effect" and strong perturbations in absorption peak of complexes as depicted in Figs. 3 and 4 (and for complex **3**, Supplementary Information fig. S2 and S3). As evident from above absorption titration, both the electrostatic binding as well as steric effects play an eminent role in the determining the binding potential of these analogous complexes with DNA, so the binding of the complexes **1** and **2** towards nucleotides is also governed by these interactions. The hyperchromic effect in the absorption spectra of the complexes indicates an electrostatic outside binding of the complexes with nucleotides owing to the

Table 1
The binding constant (K_b) values of complexes **1**, **2** and **3** with the CT-DNA (mean standard deviation of ±0.04).

Complex	K_b (M^{-1})	% Hyperchromism	Red shift (nm)
1	2.16 × 10^4	32	06
2	3.47 × 10^4	45	05
3	4.60 × 10^3	20	05

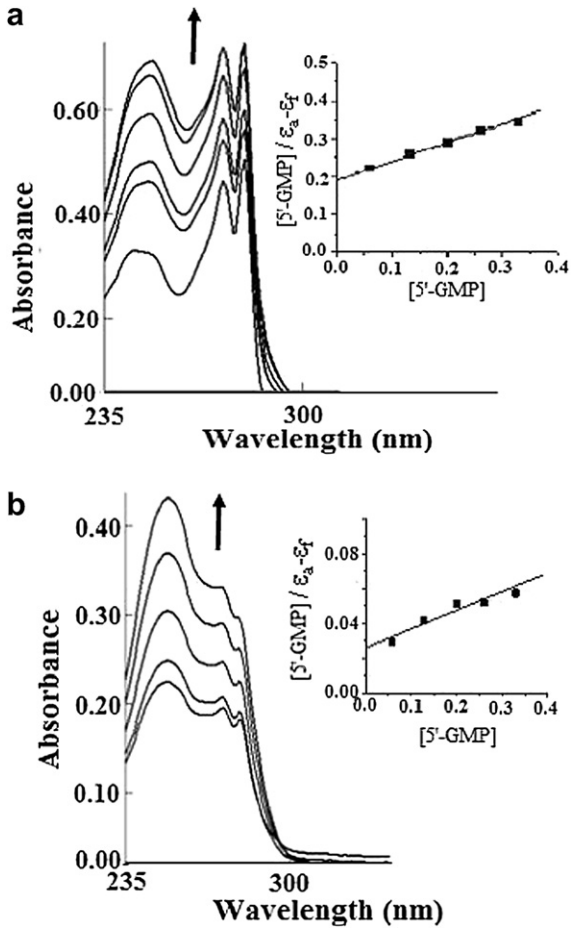

Fig. 3. Absorption spectral traces of complexes (a) **1** and (b) **2** upon addition of 5′-GMP. Inset: Plots of [5′-GMP]/$\varepsilon_a-\varepsilon_f$ vs [5′-GMP] for the titration of 5′-GMP with complexes. [Complex] = 1.3×10^{-4} M, [5′-GMP] = 0–0.33×10^{-4} M.

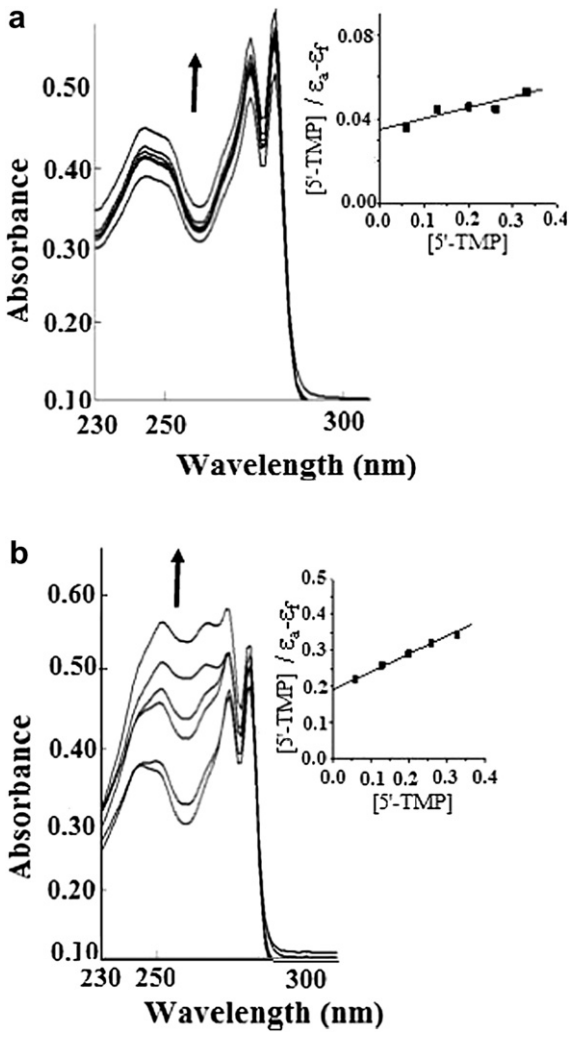

Fig. 4. Absorption spectral traces of complexes (a) **1** and (b) **2** upon addition of 5′-TMP. Inset: Plots of [5′-TMP]/|$\varepsilon_a-\varepsilon_f$| vs [5′-TMP] for the titration of 5′-TMP with complexes. [Complex] = 1.3×10^{-4} M, [5′-TMP] = 0–0.50×10^{-4} M.

presence of Sn(IV) moiety which exerts predominate phosphate binding of the complexes with nucleotide. Moreover, as observed from the binding constant data (Table 2), the interaction of complexes **1** and **2** with 5′-GMP produces more pronounced changes in the absorption spectra as compared to 5′-TMP showing a clear preference of binding of the complexes with 5′-GMP.

To further understand the selectivity of the complex **2** owing to its stronger binding with the CT-DNA and to the strong perturbations induced in the absorption spectra when treated with nucleotide 5′-GMP, we have carried out ^{1}H and ^{31}P NMR interaction of the complex with 5′-GMP. The ^{1}H NMR spectrum of the 5′-GMP after addition of the complex **2** shows no significant chemical shift differences (Fig. 5). The absence of such shift of H8 signal suggests non-involvement of the nucleobase in complex binding thus, precluding the base specific interactions with the complex. Slight shift of free ribose protons of 5′-GMP after interaction with complex **2** from 5.8 to 3.8 ppm to 5.7–3.9 ppm indicate the binding of the Sn(IV) complex through O_2' and O_3' atoms of the sugar moiety owing to its high affinity for the backbone binding. Thus, the ^{1}H NMR studies indicates an electrostatic binding mode of complex **2** with 5′-GMP. Additional evidence for the selective and specific binding of Sn(IV) complex with the phosphate group of 5′-GMP was provided by ^{31}P NMR. There was significant upfield shift of the ^{31}P signal of free 5′-GMP from 3.73 to 2.10 ppm which corresponds to a strong binding exhibited by the complex **2** to the phosphate group of the mononucleotide [44]. These observations provide a definitive affirmation of phosphate selectivity of complex with biomolecules (CT-DNA and 5′-GMP).

3.3. Fluorescence studies

In the absence of DNA, complex **1**–**3** emit weak luminescence in Tris–HCl buffer at ambient temperature, with a fluorescence maximum centered at 710 nm when excited with a wavelength of 354 nm. Upon increasing DNA from 0 to 0.50×10^{-4} M, the enhancement in the emission intensity of the complexes **1** and **2** was observed as depicted in Fig. 6 (and for complex **3**, Supplementary Information fig. S4). This observed enhancement in the emission intensity results from shielding effect of these complexes

Table 2
The comparative binding constant (K_b) values of complexes **1**, **2** and **3** with the 5′-GMP and 5′-TMP (mean standard deviation of ±0.07).

Complex	K_b(M^{-1})		Monitored at (nm)	% Hyperchromism
	5′-GMP	5′-TMP		
1	3.03×10^4	0.40×10^4	246	36
2	4.80×10^4	1.51×10^4	246	48
3	0.28×10^4	0.16×10^4	246	23

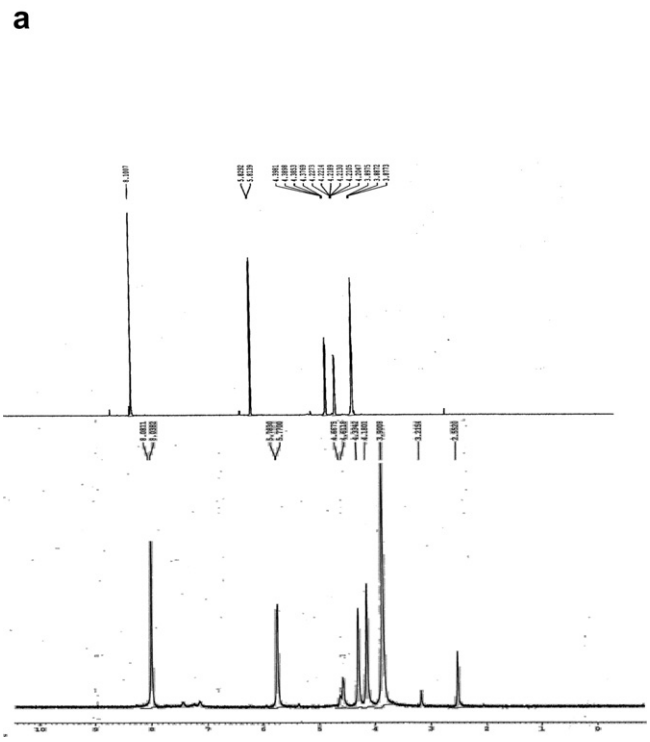

Fig. 5a. ^{1}H NMR spectra of (a) 5′-GMP alone and (b) the reaction of complex **2** (2.5 mmol) with 5′-GMP (5 mmol) at 25 °C.

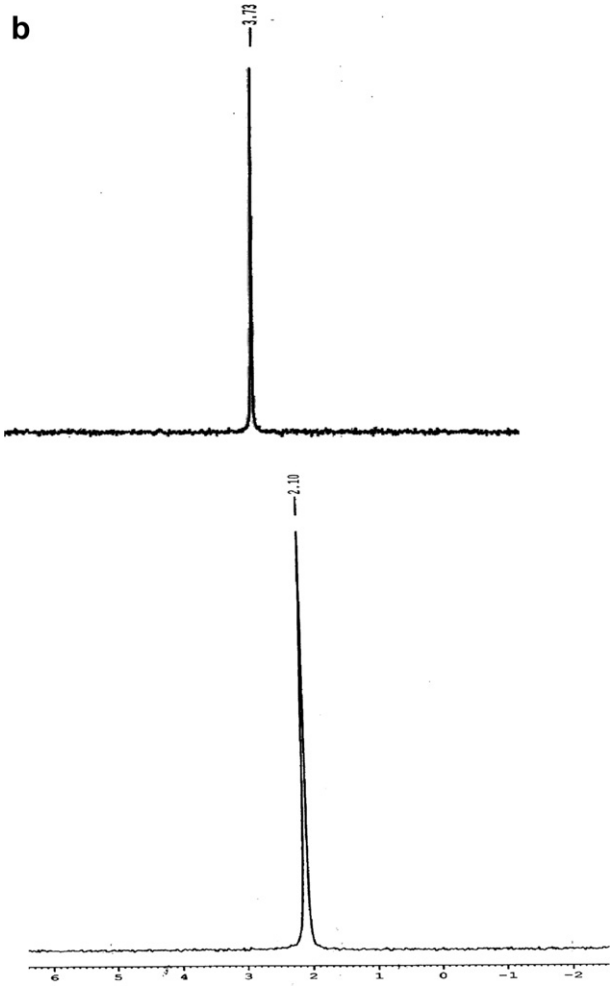

Fig. 5b. ^{31}P NMR spectra of (a) 5′-GMP and (b) the reaction of complex **2** (2.5 mmol) with 5′-GMP (5 mmol) at 25 °C.

as a consequence of their unspecific binding to the low affinity outer sphere of DNA polyanionic phosphate backbone. However, another possibility envisioned for such an increase is the effective shielding of these outer sphere complexes to the metal complexes intercalated inside the DNA pockets [45]. Generally there is interplay between electrostatic and hydrophobic interactions; even in systems in which intercalation is evident. The degree to which hydrophobic interactions predominate over electrostatic is likely to be dictated by structural, geometric, and charge considerations for the binding molecule. Since, the complex **2** displays structural variability as compared to **1** and **3**, the partial intercalative hydrophobic interaction along with electrostatic binding predominates for the complex. The propensity to CT-DNA of the complexes follows the order **2** > **1** > **3**. The values of the binding constant, K gave similar trend of the DNA binding propensity as observed in case of absorption spectral studies (Table 3).

Steady-state emission quenching experiments were performed by using anionic quencher, $[Fe(CN)_6]^{4-}$, which has been found to be able to distinguish between the binding modes of the complex with DNA [46,47]. Upon addition increasing CT-DNA, the quenching of the fluorescence intensity was observed for the complexes **1**–**3**. It is speculated that intercalated chromophores are less accessible to quenching by quencher due to electrostatic repulsion between the highly negatively charged DNA and anionic quencher [48] whereas compounds which are bound at the DNA surface (groove binding or electrostatic binding) are more accessible and therefore, the emission from these molecules can be quenched more efficiently. The fluorescence-quenching plots of DNA-bound quencher by complexes **1** and **2** are shown in Fig. 7 and for complex **3** in supplementary information fig. S5, which illustrate that quenching phenomena of DNA-bound $[Fe(CN)_6]^{4-}$ by complexes **1**–**3** are in good agreement with the linear Stern–Volmer equation. However, in presence of DNA the slope of the plot of was remarkably decreased (Table 4). These results corroborate well with the observations of absorption titrations indicating that the complex **2** bind with higher affinity towards DNA as compared to other complexes **1** and **3** predominantly via, electrostatic interactions.

3.3.1. *Effect of ionic strength*

In order to validate the probable binding mode between the molecule and DNA, fluorescence titrations were carried out under the conditions of increasing ionic strength (0–0.50 × 10^{-4} M) through added amounts of NaCl. The fluorescence intensity of complexes **1**–**3** was appreciably quenched with increasing ionic strength (Fig. 8 and supplementary information fig. S6) [49,50]. This change in CT-DNA is in favor of the electrostatic binding of complexes **1** and **2** with CT-DNA. As evident from, the effect of salt concentration on complex **2**-DNA system was more pronounced in case of complex **2** than the other complexes revealing a greater potency for DNA binding.

3.3.2. *Effect of phosphate group*

The fluorescence intensity of complexes **1**–**3** increases with increase in the K_2HPO_4 concentration (Fig. 9 and supplementary information fig. S7). This observation provides supportive evidence for electrostatic interaction of the complexes binding preferentially to the phosphate group of DNA double helix. The spectra depicts that the interaction of complex **2** is relatively strong than complexes **1** which is consistent with the absorption spectral studies.

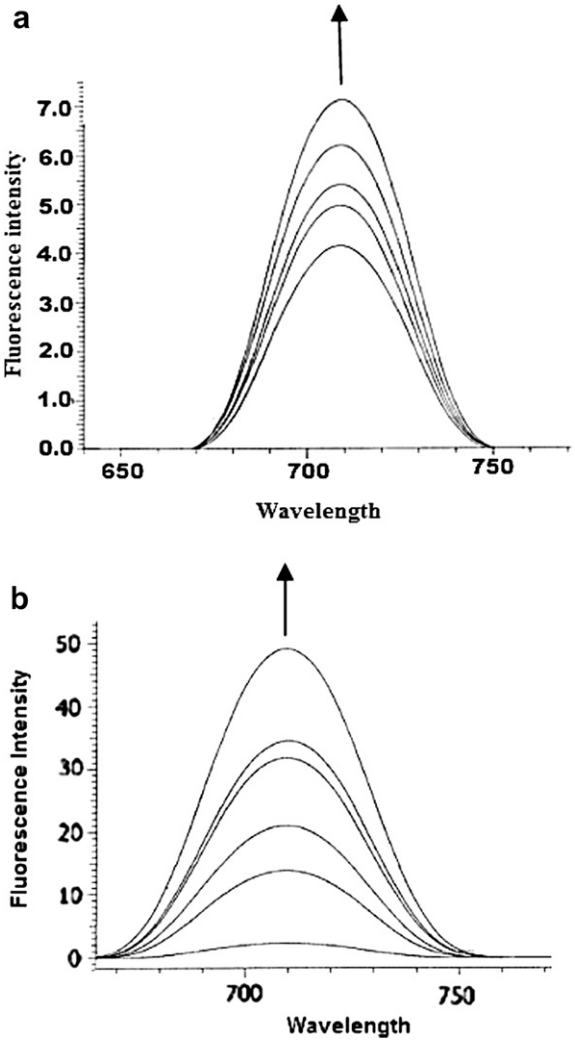

Fig. 6. Emission spectra of complexes (a) **1** and (b) **2** in Tris–HCl buffer (pH = 7.2) in the absence and presence of CT-DNA. [Complex] = 1.3 × 10^{-4} M, [DNA] = 0–0.50 × 10^{-4} M. Arrows indicate the change in emission intensity upon increasing the DNA concentration.

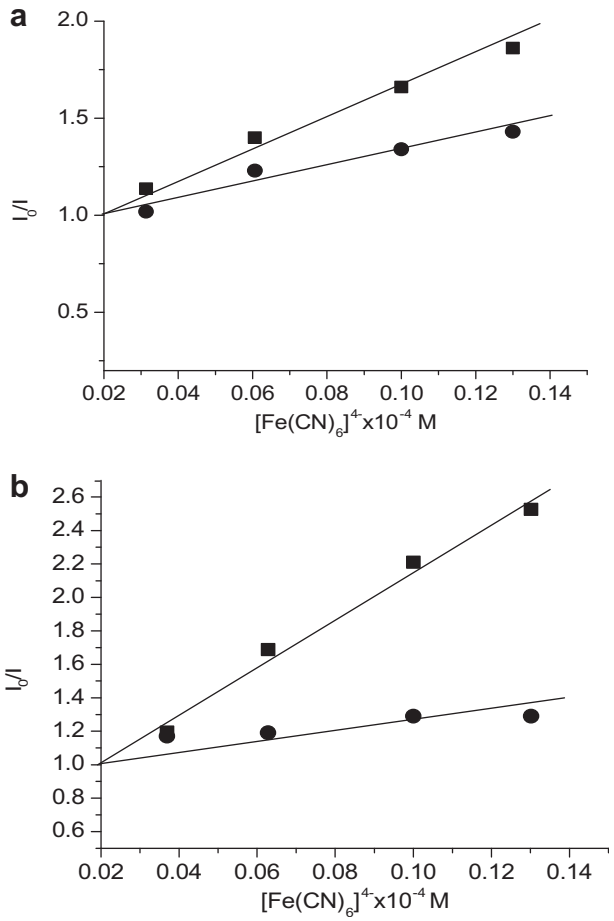

Fig. 7. Emission quenching curves of (a) **1** and (b) **2** in the absence of CT-DNA (■) and in the presence of CT-DNA (●). [Complex] = 1.3 × 10^{-4} M, [DNA] = 1.0 × 10^{-4} M.

3.4. Circular dichroism

The circular dichroism pattern observed for CT-DNA provide further and definitive confirmation of the probable mode of CT-DNA binding of complexes **1**–**3** which is depicted by the perturbation induced in the DNA morphology upon the binding of complexes to CT-DNA. The two bands of CT-DNA are a net result of excitation coupling interaction of bases which depend on the skewed orientation on the CT-DNA backbone [51]. On incubation of the complexes with CT-DNA, moderate changes in both the positive and negative bands of CT-DNA were observed. The multifaceted binding mode observed for complex **2** promotes its higher binding towards the DNA such that effective screening of the negative charge on the N7 base site as well as phosphate oxygen, simultaneously along the phosphate backbone is observed which support a trans conformational change of the DNA double helical conformation [52]. It has been speculated that the electrostatic components of interactions are effective in bringing about such trans conformational changes. Further transformation of the DNA structure proceeds by removal of labile groups attached in the complexes which removes the water from the base sites and grooves of DNA helix resulting in effective binding of the complex to DNA. The CD spectrum of DNA shows a significant decrease in intensity of positive band upon addition of the complex **2** which reveal a right handed conformational change of the DNA double helix possibly due to its partial intercalative binding of the complex. In contrast, the complexes **1** and **3** (Fig. 10) exhibit less pronounced CD spectral changes in the positive ellipticity band. However, on addition of the complexes, no appreciable change in the negative helicity band of CT-DNA was observed for all the complexes. The

Table 3
Emission properties of complexes **1**, **2** and **3** bound to CT-DNA (mean average deviation of ±0.02).

Complex	Emission (nm)	Excitation (nm)	Monitored at (nm)	K(M^{-1})
1	442	354	710	2.0 × 10^4
2	446	354	710	4.2 × 10^4
3	442	354	710	1.4 × 10^4

Table 4
Emission quenching of CT-DNA bound $[Fe(CN)_6]^{4-}$ by complexes **1**, **2** and **3** (mean average deviation of ±0.02).

Complex	Emission (nm)	Excitation (nm)	Monitored at (nm)	K_{sv1}	K_{sv2}
1	442	354	710	2.57 × 10^4	1.28 × 10^4
2	446	354	710	1.0 × 10^4	5.7 × 10^4
3	442	354	710	3.14 × 10^4	1.42 × 10^4

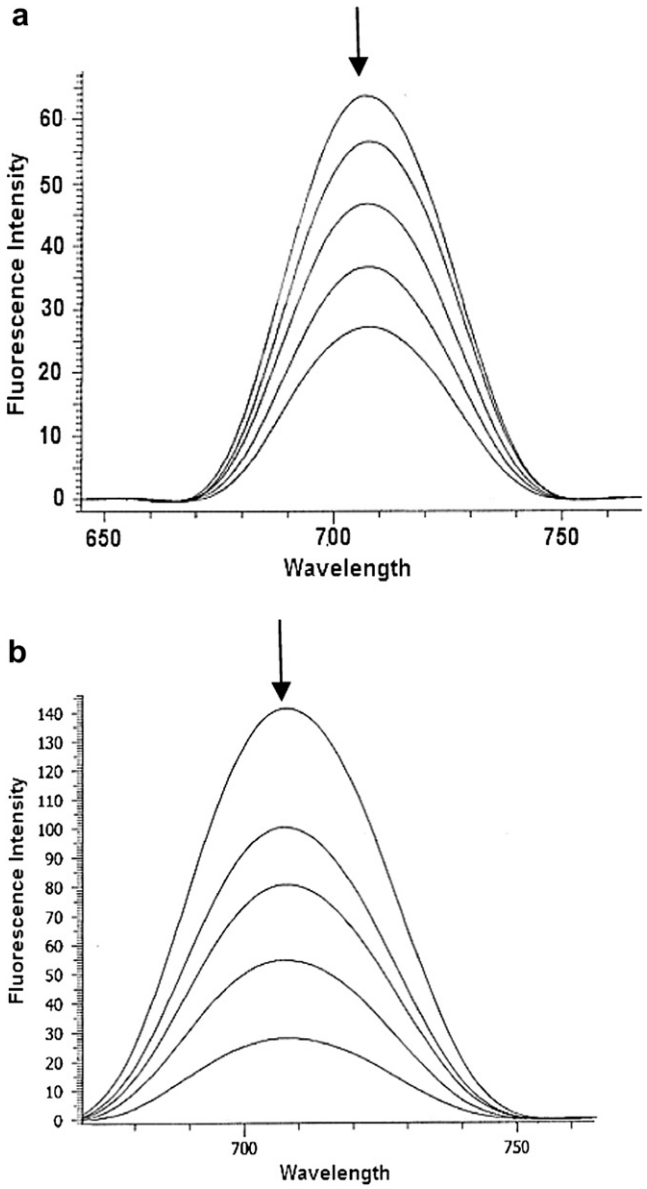

Fig. 8. Effect of different concentration of NaCl on the fluorescence spectra of complexes (a) **1** and (b) **2** where [Complex] = 1.3×10^{-4} M with [DNA] = 1.0×10^{-4} M. Arrow indicate the gradual decrease of emission intensity as a function of NaCl concentration.

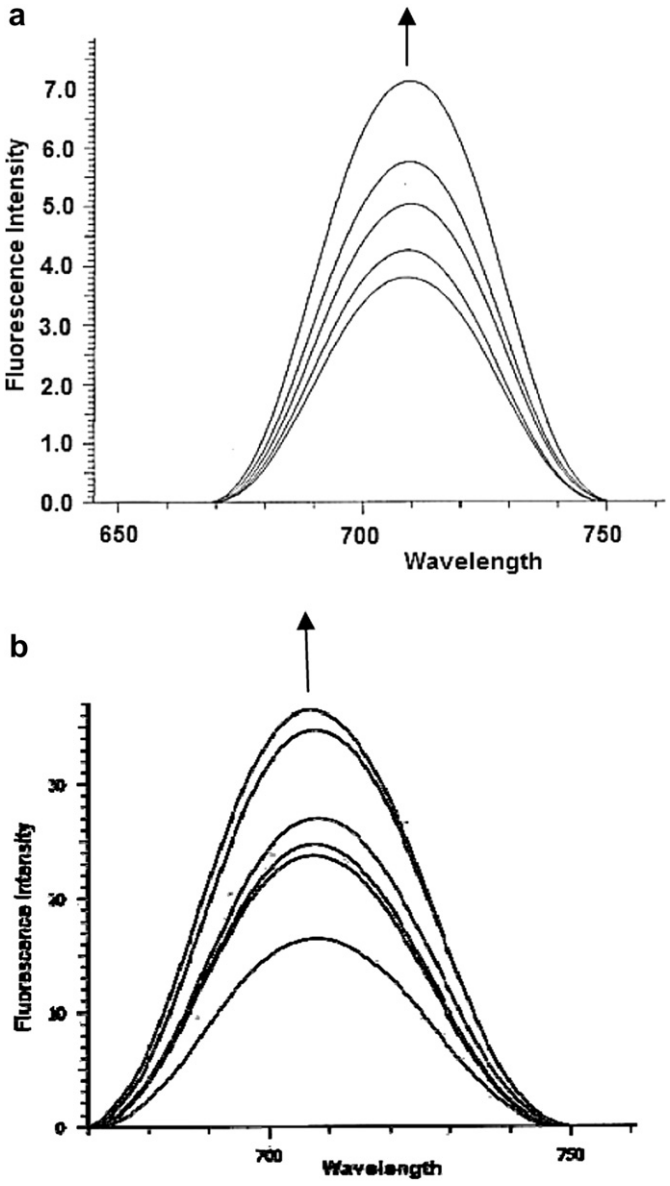

Fig. 9. Effect of increasing concentration of K_2HPO_4 on the fluorescence intensity of the complexes (a) **1** and (b) **2**. [Complex] = 1.0×10^{-4} M with [CT-DNA] = 1.20×10^{-4} M. Arrow indicate the gradual decrease of emission intensity as a function of K_2HPO_4 concentration.

observation is in accordance with the above spectroscopic studies revealing avid binding of complex **2** as compared to complexes **1** and **3**.

3.5. Viscosity measurements

The relative viscosity of CT-DNA (1.20×10^{-4} M) in presence of varying amounts of complexes **1**–**3** in the [complex]/[DNA] (r) ratio of 0.00–0.40 with an interval of 0.1 are shown in Fig. 11. Complex **2** interacts with the CT-DNA more strongly and deeply than other complexes **1** and **3**, leading to the greater decrease in viscosity of the DNA with an increasing value of r = 0.00–0.20 followed by a substantial increase in the viscosity of the CT-DNA from r = 0.20–0.40. Firstly, the initial decrease in the relative viscosity of CT-DNA indicate non-intercalative interaction presumably electrostatic interactions of the complexes with DNA which would produce bends or kinks in the DNA strand and hence, diminish its effective length along with its viscosity. Secondly, when the r ratios were increased from 0.20 to 0.40, rapidly increasing viscosity was observed which indicates the partial intercalative binding mode of the complexes and supports an electrostatic binding mode together with some partial intercalative interactions for the complexes **1** and **2** [53]. However, the higher reduction at r = 0.00–0.20 and the higher enhancement at r = 0.20–0.40 in the DNA viscosity for complex **2** compared to **1** recommends that former complex reveals a greater DNA binding potential than the latter. However, in contrast to this observation, there is a gradual decrease in the viscosity of DNA on addition of complex **3** supporting only an electrostatic association of the complex towards CT-DNA. These results obtained from viscosity studies are consistent with those obtained from above spectroscopic studies.

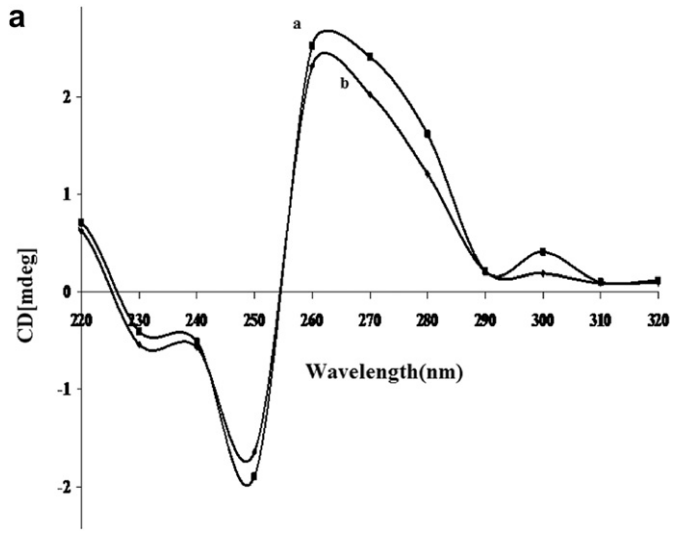

Fig. 10a. CD spectra of (a) CT-DNA alone (b) CT-DNA in presence of metal complex **1** in Tris–HCl buffer at 25 °C. [Complex] = 1.0×10^{-4} M, [DNA] = 1.20×10^{-4} M.

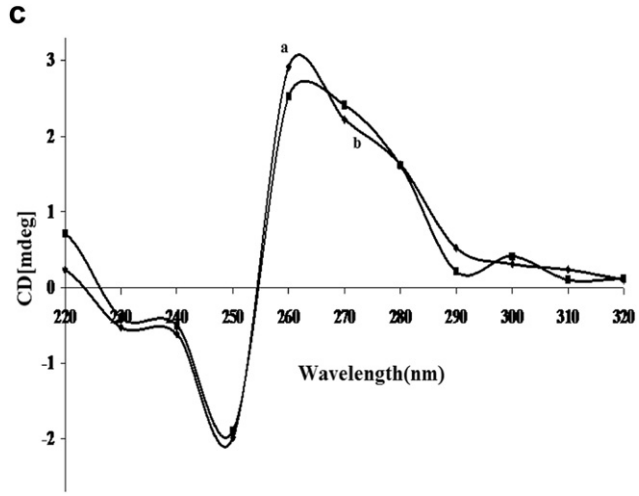

Fig. 10c. CD spectra of (a) CT-DNA alone (b) CT-DNA in presence of metal complex **3** in Tris–HCl buffer at 25 °C. [Complex] = 1.0×10^{-4} M, [DNA] = 1.20×10^{-4} M.

4. Conclusions

In this paper, we have attempted to unravel the binding behavior of the complexes **1**–**3** with CT-DNA by employing various spectroscopic and biophysical methods. The results suggest a multifaceted mode of binding of the complexes **1** and **2** with CT-DNA i.e. electrostatic binding mode in addition to partial intercalative interactions owing to the presence of planar architectures within the molecule as evidenced by absorption titrations and fluorescence studies. The complex **2** binds to CT-DNA more strongly than complexes **1** and **3**. Further studies of the complexes **1**–**3** with mononucleotides 5′-GMP and 5′-TMP by employing UV–visible absorption titrations as well as ^{1}H and ^{31}P NMR lends a strong affirmation of electrostatic interaction of complexes with biomolecules. The CD spectra reveal higher perturbations in DNA helical conformation for complex **2** as compared to other complexes **1** and **3** suggestive of its higher binding affinity with DNA leading to strong conformational changes in the double helical structure of CT-DNA. The above DNA binding results were in agreement with viscometric studies which supports two probable mode of associations of the complexes **1** and **2** with DNA viz; electrostatic in addition to some partial intercalative interactions, while the complex **3** binds only via an electrostatic interaction with DNA.

5. Experimental

5.1. Materials and method

All reagents were of the best commercial grade and were used without further purification. 1,2-diaminobenzene (Sigma), L(+)-tartaric acid (Merck), dimethyltin(IV)dichloride (Sigma), trimethyltin(IV)chloride (Sigma), Tris(hydroxymethyl)aminomethane or Tris buffer (Sigma) were used as received. Disodium salt of Calf thymus DNA (CT-DNA), guanosine 5′-monophosphate disodium salt (5′-GMP) and thymidine 5′-monophosphate disodium salt (5′-TMP) were purchased from Sigma Chemical Co and Fluka, respectively and were stored at 4 °C.

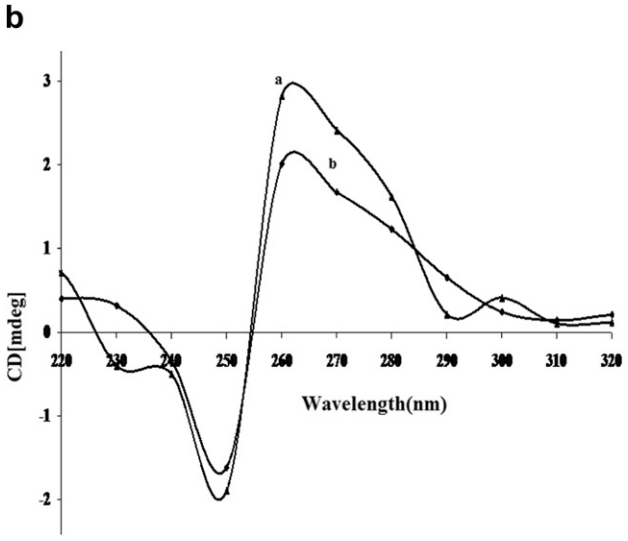

Fig. 10b. CD spectra of (a) CT-DNA alone (b) CT-DNA in presence of metal complex **2** in Tris–HCl buffer at 25 °C. [Complex] = 1.0×10^{-4} M, [DNA] = 1.20×10^{-4} M.

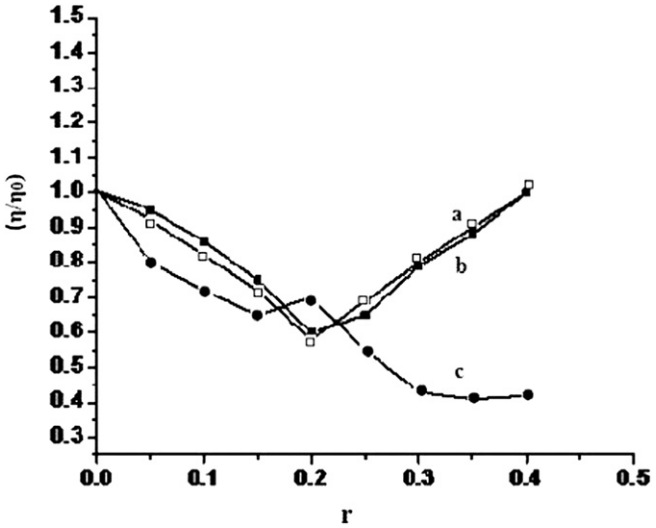

Fig. 11. Effect of increasing amount of complexes (a) **1** (b) **2** and (c) **3** on the relative viscosity of CT-DNA. [DNA] = 1.20×10^{-4} M, [Complex] = 0–1.0×10^{-4} M.

5.2. Physical measurements

The elemental analyses were determined using Carlo Erba Analyzer Model 1108. Molar conductance was measured at room temperature on a Digsun Electronic conductivity Bridge. Infrared (IR) spectra were recorded on an Interspec 2020 FTIR spectrometer. Electronic spectra were recorded on UV-1700 PharmaSpec UV–vis spectrophotometer (Shimadzu). The ^{1}H and ^{13}C NMR spectra were obtained on a Bruker DRX-400 spectrometer. Optical rotations of chiral complexes were determined on a Polarimeter Rudolf Autopol III at 25 °C using the sodium D line in DMSO. ESI-MS spectra were recorded on Micromass Quattro II triple quadrupole mass spectrometer.

5.3. DNA binding experiments

DNA binding experiments which include absorption spectral traces, luminescence and circular dichoric experiments conformed to the standard methods [54–57] and practices previously adopted by our laboratory [22,58]. While measuring the absorption spectra an equal amount of DNA was added to both the compound solution and the reference solution to eliminate the absorbance of the CT-DNA itself, and the CD contribution by the CT-DNA and Tris buffer was subtracted through base line correction.

5.4. Syntheses

The synthesis of the ligand was a straight forward Phillips condensation reaction and the new organotin(IV) complexes **1**–**3** were prepared by the coordination of ligands to the central metal ion via nitrogen and oxygen donor atom. Nitrogen atoms participate through the coordinate linkages, while oxygen atom is involved in coordination under release of HCl in 1:1 stoichiometric ratio (Scheme 1). These complexes were stable at room temperature and soluble in various organic solvents such as methanol, ethanol and DMSO. Molar conductance values of complexes in methanol were recorded as 59, 34 and 37 Ω^{-1} cm^2 mol^{-1} for the complexes **1**, **2** and **3**, respectively, suggesting their non-electrolytic nature. The geometry of tin was ascertained by ^{119}Sn NMR spectra which revealed a pentacoordinate geometry for complexes **1** and **3**, while hexacoordinate environment for complex **2**.

5.4.1. Synthesis of ligand, $[C_{16}H_{14}N_4O_2]$ (**L**)

The ligand was prepared by reaction of 1,2-diaminobenzene (4.6 g, 40 mmol) and L(+)-tartaric acid (3.0 g, 20 mmol), according to the procedure reported earlier [30]. Yield, 65%. m.p. 270 ± 2 °C, Anal. Calc. for $[C_{16}H_{14}N_4O_2]$ (%): C 65.30; H 4.79; N 19.04: found % C 65.32; H 4.81; N 19.01. $[\alpha]_D^{25} = +110$, ESI-MS (*m*/*z*): 295 $[C_{16}H_{14}N_4O_2]$.

Selected IR data on KBr (ν/cm^{-1}): 3322 υ(OH); 1623 υ(C=N); 1227 υ(C–O); 740 υ(Ar). UV–vis (MeOH) [λ_{max}/nm]: 206, 247, 278. ^{1}H NMR (DMSO-d_6, ppm): 5.49–5.67 (–CH); 6.41(–OH); 7.10–7.52 (Aromatic-H). ^{13}C NMR (DMSO-d_6, ppm): 155 (C=N); 115–121 (Ar–C); 71 (C–O).

5.4.2. Synthesis of $[C_{18}H_{19}N_4O_2SnCl]$ (**1**)

To a stirring solution of dimethyltin(IV)dichloride (1.07 g, 5 mmol) in methanol (20 ml) was added the ligand $[C_{16}H_{14}N_4O_2]$ (1.47 g, 5 mmol). The reaction mixture was refluxed at 80 °C with constant stirring on the rota mantle for 4 h and then allowed to stand at room temperature overnight (25 °C). Slow evaporation of the resulting mixture afforded white amorphous complex. The above complex was washed with hexane and dried in vacuo. Yield, 56%. m.p. 210 ± 2 °C. Anal. Calc. for $[C_{18}H_{19}N_4O_2SnCl]$ (%): C 45.27; H 4.01; N 11.73: found % C 45.30; H 4.1; N 11.76. $[\alpha]_D^{25} = +193$, ESI-MS (*m*/*z*): 478 $[C_{18}H_{19}N_4O_2Sn]$. Molar Conductance, Λ_M (1×10^{-3} M, MeOH): 59 Ω^{-1} cm^2 mol^{-1} (non-electrolyte). Selected IR data (ν/cm^{-1}): 3220 υ(OH); 3042 υ(NH); 1625 υ(C=N); 1222 υ(C–O); 759 υ(Ar); 557 υ(Sn–C); 470 υ(Sn–N); 435 υ(Sn–O); 256 υ(Sn–Cl). UV–vis (MeOH) [λ_{max}/nm]: 210, 245, 275. ^{1}H NMR (DMSO-d_6, ppm): 5.9 (–CH); 6.4 (–OH); 7.1–7.8 (Aromatic-H). ^{13}C NMR (DMSO-d_6, ppm): 154 (C=N); 114–128 (Ar–C); 70 (C–O); 10–12 (–CH_3). ^{119}Sn NMR (DMSO-d_6, ppm): −189.

5.4.3. Synthesis of $[C_{28}H_{23}N_4O_2SnCl]$ (**2**)

The complex **2** was prepared from diphenyltin(IV)dichloride (1.71 g, 5 mmol) and ligand $[C_{16}H_{14}N_4O_2]$ (1.47 g, 5 mmol) according to the procedure described above for complex **1**. Yield, 64%. m.p. 215 ± 2 °C. Anal. Calc. for $[C_{28}H_{23}N_4O_2SnCl]$ (%): C 55.89; H 3.85; N 9.31: found % C 55.85; H 3.86; N 9.34. $[\alpha]_D^{25} = +120$, ESI-MS (*m*/*z*): 604 $[C_{28}H_{23}N_4O_2SnCl+2H]$. Molar Conductance, Λ_M (1×10^{-3} M, MeOH): 34 Ω^{-1} cm^2 mol^{-1} (non-electrolyte). Selected IR data (ν/cm^{-1}): 3208 υ(OH); 3046 υ(NH); 1625 υ(C=N); 1226 υ(C–O); 747

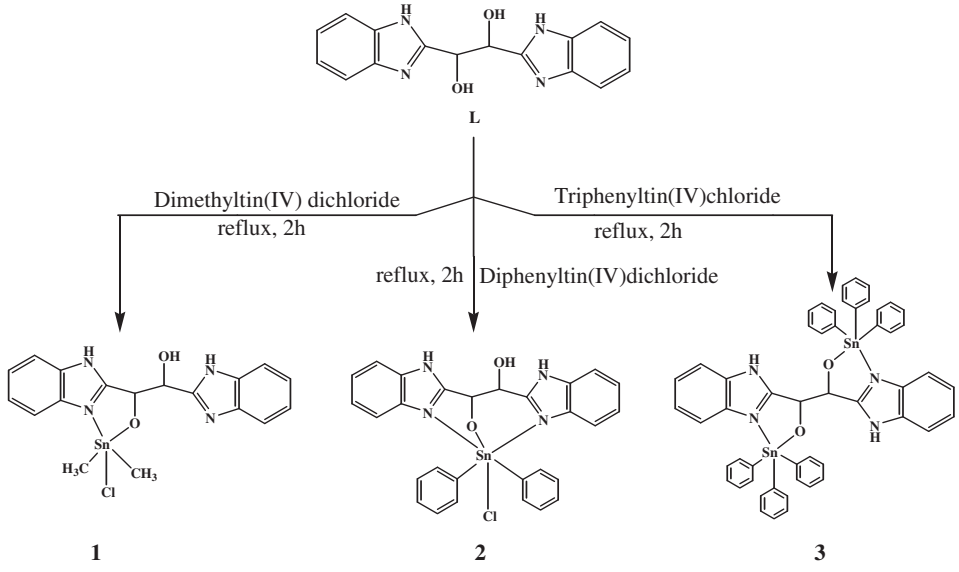

Scheme 1. Schematic representation of the formation of complexes **1**, **2** and **3**.

υ(Ar); 588 υ(Sn–C); 472 υ(Sn–N); 435 υ(Sn–O); 263 υ(Sn–Cl). UV–vis (MeOH) [λ_{max}/nm]: 207, 244, 274. ^{1}H NMR (DMSO-d_6, ppm): 5.5–5.4 (–CH); 6.6 (–OH); 7.1–7.9 (Aromatic-H). ^{13}C NMR (DMSO-d_6, ppm): 154 (C=N); 114–136 (Ar–C); 69 (C–O). ^{119}Sn NMR (DMSO-d_6, ppm): −586.

*5.4.4. Synthesis of [$C_{52}H_{42}N_4O_2Sn_2$] (**3**)*

The complex **3** was prepared from triphenyltin(IV)chloride (1.92 g, 5 mmol) and ligand [$C_{16}H_{14}N_4O_2$] (1.47 g, 5 mmol) according to the procedure described above. Yield, 69%. m.p. > 300 °C (decompose). Anal. Calc. for [$C_{52}H_{42}N_4O_2Sn_2$] (%): C 62.94; H 4.27; N 5.65: found % C 62.86; H 4.22; N 5.66. $[\alpha]_D^{25} = +90$, ESI-MS (*m*/*z*): 1009 [$C_{52}H_{42}N_4O_2Sn_2 + 0.5CH_3OH$]. Molar Conductance, Λ_M (1×10^{-3} M, MeOH): 37 Ω^{-1} cm^2 mol^{-1} (non-electrolyte). Selected IR data (ν/cm^{-1}): 1621 υ(C=N); 3062 υ(NH); 1222 υ(C–O); 735 υ(Ar); 561 υ(Sn–C); 452 υ(Sn–N); 446 υ(Sn–O). UV–vis (MeOH) [λ_{max}/nm]: 207, 245, 275. ^{1}H NMR (DMSO-d_6, ppm): 5.5–5.8 (–CH); 7.1–7.9 (Aromatic-H). ^{13}C NMR (DMSO-d_6, ppm): 155 (C=N); 114–136 (Ar–C); 70 (C–O). ^{119}Sn NMR (DMSO-d_6, ppm): −222.

Acknowledgements

The authors are highly indebted to the Regional Sophisticated Instrumentation Center (RSIC), Central Drug Research Institute, Lucknow, India for providing CHN analysis data, ESI-Mass and polarimetry, Sophisticated Analytical Instrumentation Facility (SAIF), Panjab University, Chandigarh for providing the NMR spectra. Thanks are also due to Dr. Rizwan H. Khan, Interdisciplinary Biotechnology Unit, AMU, Aligarh for providing the CD facility.

Appendix. Supplementary data

Supplementary data associated with this article can be found, in the online version, at doi:10.1016/j.jorganchem.2011.08.007.

References

[1] B. Rosenberg, Nature 222 (1969) 385–386.
[2] (a) J. Reedijk, Chem. Commun. (1996) 801–806;
(b) J. Reedijk, J.M. Teuben, in: B. Lippard (Ed.), Cisplatin, Chemistry and Biochemistry of a Lead Anticancer Drug, Wiley, Weinheim, Germany, 1996, pp. 339–362.
[3] A. Alama, B. Tasso, F. Novelli, F. Sparatore, Drug Discov. Today 14 (2009) 500–508.
[4] A.J. Crowe, Drugs Fut. 12 (1987) 255–275.
[5] S. Shuja, A. Shah, Z. Rehman, N. Muhammad, S. Ali, R. Qureshi, N. Khalid, A. Meetsma, Eur. J. Med. Chem. 45 (2010) 2902–2911.
[6] N. Muhammad, A. Shah, Z. Rehman, S. Shuja, S. Ali, R. Qureshi, A. Meetsma, M.N. Tahir, J. Organomet. Chem. 694 (2009) 3431–3437.
[7] Z. Rehman, A. Shah, N. Muhammad, S. Ali, R. Qureshi, I.S. Butler, Eur. J. Med. Chem. 44 (2009) 3986–3993.
[8] Z. Rehman, A. Shah, N. Muhammad, S. Ali, R. Qureshi, I.S. Butler, J. Organomet. Chem. 694 (2009) 1998–2004.
[9] S.K. Hadjikakou, N. Hadjiliadis, Coord. Chem. Rev. 253 (2009) 235–249.
[10] (a) K.H. Thompson, C. Orvig, Science 300 (2003) 936–939;
(b) J. Reedijk, Proc. Natl. Acad. Sci. U.S.A 7 (2003) 3611–3616.
[11] (a) S.C. Stinson, Chem. Eng. News 79 (2001) 45–56;
(b) Q. Xiaogang, J.O. Trent, I. Fokt, W. Priebe, J.B. Chaires, Proc. Natl. Acad. Sci. U.S.A 97 (2000) 12032–12037.
[12] S. Grassmann, B. Sadek, X. Ligneau, S. Elz, C.R. Ganellin, J.M. Arrang, J.C. Schwartz, H. Stark, W. Schunack, Eur. J. Pharm. Sci. 15 (2002) 367–378.
[13] J.E. Richter, Am. J. Gastroenterol. 92 (1997) 30–34.
[14] S.M. Sondhi, N. Singh, M. Johar, A. Kumar, Bioorg. Med. Chem. 13 (2005) 6158–6166.
[15] B. Can-Eke, M.O. Puskullu, E. Buyukbingol, M. Iscan, Chem.-Biol. Interact. 113 (1998) 65–77.
[16] R.W. Burli, D. McMinn, J.A. Kaizerman, W. Hu, Y. Ge, Q. Pack, V. Jiang, M. Gross, M. Garcia, R. Tanaka, H.E. Moser, Bioorg. Med. Chem. Lett. 14 (2004) 1253–1257.
[17] A.W. White, N.J. Curtin, B.W. Eastman, B.T. Golding, Z. Hostomsky, S. Kyle, J. Li, K.A. Maegley, D.J. Skalitzy, S.E. Webber, X.H. Yu, R.J. Griffin, Bioorg. Med. Chem. Lett. 14 (2004) 2433–2437.
[18] L. Garuti, M. Roberti, M. Malagoli, T. Rossi, M. Castelli, Bioorg. Med. Chem. Lett. 10 (2000) 2193–2195.
[19] A. Hori, Y. Imaeda, K. Kubo, M. Kusaka, Cancer Lett. 183 (2002) 53–60.
[20] M.J. Hannon, Chem. Soc. Rev. 36 (2007) 280–295.
[21] M. Chauhan, F. Arjmand, J. Organomet. Chem. 692 (2007) 5156–5164.
[22] M. Chauhan, K. Banerjee, F. Arjmand, Inorg. Chem. 46 (2007) 3072–3082.
[23] G.F. deSouza, V.M. Deflon, M.T.P. Gambardella, R.H.P. Francisco, J.D. Ardisson, E. Niquet, Inorg. Chem. 45 (2006) 4518–4525.
[24] A. Tavman, B. Ülküseven, Trans. Met. Chem. 25 (2000) 324–328.
[25] M.A. Abdellah, S.K. Hadjikakou, N. Hadjiliadis, M. Kubicki, T. Bakas, N. Kourkoumelis, Y.V. Simos, S. Karkabounas, M.M. Barsan, I.S. Butler, Bioinorg. Chem. Appl. 2009 542979 (2009) 1–12.
[26] E. Katsoulakou, M. Tiliakos, G. Papaefstathiou, A. Terzis, C. Raptopoulou, G. Geromichalos, K. Papazisis, R. Papi, A. Pantazaki, D. Kyriakidis, P. Cordopatis, E.M. -Zoupa, J. Inorg. Biochem. 102 (2008) 1397–1405.
[27] L. Tian, Z. Sheng, X. Zheng, Y. Sun, Y. Yu, B. Qian, X. Liu, Appl. Organomet. Chem. 20 (2006) 74–80.
[28] C. Ma, Y. Han, R. Zhang, D. Wang, Dalton Trans. (2004) 1832–1840.
[29] F. Marchetti, C. Pettinari, A. Cingolani, R. Pettinari, M. Rossi, F. Caruso, J. Organomet. Chem. 645 (2002) 134–145.
[30] K. Isele, V. Broughton, C.J. Matthews, A.F. Williams, G. Bernardinelli, P. Franz, S. Decurtins, Dalton Trans. (2002) 3899–3905.
[31] H. Xu, K. Zheng, Y. Chen, Y.Z. Li, L.J. Lin, H. Li, P.X. Zhang, L.N. Ji, Dalton Trans. (2003) 2260–2268.
[32] L.-F. Tan, H. Chao, K.-C. Zhen, J.-J. Fei, F. Wang, Y.-F. Zhou, L.-N. Ji, Polyhedron 26 (2007) 5458–5468.
[33] T.S. Basu Baul, A. Mizar, A. Lyčka, E. Rivarola, R. Jirásko, M. Holčapek, D. deVos, U. Englert, J. Organomet. Chem. 691 (2006) 952–965.
[34] A. Sebald, Advanced Applications of NMR to Organometallic Chemistry, Solid State NMR Applications in Organotin and Organolead Chemistry. John Wiley and Sons, Chichester, U.K, 1996.
[35] C. Pettinari, in: J.C. Lindon (Ed.), Heteronuclear NMR Applications (Ge, Sn, Pb), Encyclopedia of Spectroscopy and Spectrometry, Academic Press, London, 1999.
[36] L.C. Damude, P.A.W. Dean, V. Masivannman, R.S. Srivastava, J.J. Vitali, Can. J. Chem. 68 (1990) 1323–1331.
[37] C. Pettinari, F. Caruso, N. Zaffaroni, R. Villa, F. Marchetti, R. Pettinari, C. Phillips, J. Tanski, M. Rossi, J. Inorg. Biochem. 100 (2006) 58–69.
[38] P.M. Krishna, K.H. Reddy, P.G. Krishna, G.H. Phillip, Ind. J. Chem. 46A (2007) 904–908.
[39] Q.S. Li, P. Yang, H.F. Wang, M.L. Guo, J. Inorg. Biochem. 64 (1996) 181–195.
[40] G. Han, P. Yang, J. Inorg. Biochem. 91 (2002) 230–236.
[41] S. Kashanian, N. Shahabadi, H. Roshanfekr, K. Shalmashi, K. Omidfar, Biochemistry (Moscow) 73 (2008) 929–936.
[42] A. Janscó, L. Nagy, E. Moldrheim, E. Sletten, Dalton Trans. (1999) 1587–1594.
[43] R.W. Gellert, R. Bau, in: H. Siegel (Ed.), Metal Ions in Biological Systems, Marcel Dekker, New York, 1979.
[44] L. Ghys, M. Biesemans, M. Gielen, A. Garoufis, N. Hadjiliadis, R. Willem, J.C. Martins, Eur. J. Inorg. Chem. (2000) 513–522.
[45] C. Hiort, P. Lincoln, B. Nordén, J. Am. Chem. Soc. 115 (1993) 3448–3454.
[46] C.V. Kumar, E.H. Asuncion, J.K. Barton, N.J. Turro, J. Am. Chem. Soc. 115 (1993) 8547–8553.
[47] C.V. Kumar, E.H.A. Punzalan, W.B. Tan, Tetrahedron 56 (2007) 7027–7040.
[48] M.-J.R.P. Queiroz, E.M.S. Castanheira, T.C.T. Lopes, Y.K. Cruz, G. Kirsch, J. Photochem. Photobiol. A: Chem. 190 (2007) 45–52.
[49] F.-Y. Wu, F.-Y. Xie, Y.-M. Wu, J.-I. Hong, J. Fluoresc. 18 (2008) 175–181.
[50] J.B. Lepecq, C. Paoletti, J. Mol. Biol. 27 (1967) 87–106.
[51] A. Rodger, B. Nordén, Circular Dichroism and Linear Dichroism. Oxford Chemistry Press, UK, 1997.
[52] S. Mahadevan, M. Palaniandavar, Inorg. Chim. Acta 254 (1997) 291–302.
[53] U. Chaveerach, A. Meenongwa, Y. Trongpanich, C. Soikum, P. Chaveerach, Polyhedron 29 (2010) 731–738.
[54] J. Marmur, J. Mol. Biol. 3 (1961) 208–218.
[55] M.E. Reicmann, S.A. Rice, C.A. Thomas, P. Doty, J. Am. Chem. Soc. 76 (1954) 3047–3053.
[56] A. Wolfe, G.H. Shimer, T. Meehan, Biochemistry 26 (1987) 6392–6396.
[57] J.R. Lakowiez, G. Webber, Biochemistry 12 (1973) 4161–4170.
[58] F. Arjmand, M. Aziz, Eur. J. Med. Chem. 44 (2009) 834–844.